

Sources of Configurational Entropy versus Compositional Trends in Fragility of Inorganic Glass-Forming Liquids

Sabyasachi Sen* and Hao Chen

The effect of the average network connectivity $\langle r \rangle$ on the configurational entropy S_{conf} plays a key role in governing the compositional evolution of the fragility index m for chalcogenide, silicate, and phosphate glass-forming liquids (GFLs). The effect of $\langle r \rangle$ on S_{conf} , and thus on m in chalcogenide and phosphate GFLs can be explained using the self-avoiding walk model for a chain of either chalcogen atoms (e.g., Se) or PO_4 tetrahedra, with various degrees of cross-linking. It is shown that while a disjointed chain is suitable for modeling the inverse relationship between m and $\langle r \rangle$ in chalcogenides, semiflexible chains with a higher degree of bending stiffness are more appropriate for modeling the phosphate liquids. In contrast, the silicate and aluminosilicate GFLs exhibit a fundamentally different pattern, which is indicative of S_{conf} being controlled by the structural relaxation of a dynamically percolative network via the chemical exchange between bridging and non-bridging oxygen. In contrast to silicates and phosphates, in the case of borate and germanate GFLs, the temperature dependence of the relative fractions of B or Ge atoms in multiple coordination states becomes the predominant contributor to the $\frac{dS_{\text{conf}}}{dT}$, which is consistent with their apparently anomalous trend of m increasing with $\langle r \rangle$.

“fragile,” the former (latter) being characterized by a relatively low (high) value of m .^[3]

It is now widely accepted that the origin of the non-Arrhenius behavior of viscosity of a GFL or its fragility lies in the temperature dependence of the configurational entropy S_{conf} of the liquid.^[2,4–8] According to the model by Adam and Gibbs, upon cooling, the structural relaxation time τ of a GFL increases exponentially with $1/(TS_{\text{conf}})$.^[4] This strong dependence of τ on S_{conf} indicates that only a modest change of the latter with temperature can account for the strongly non-Arrhenius behavior of the former in some GFLs. However, the nature and source of S_{conf} in various GFLs are not always clear. In this study, we attempt to model and explain the general trends in the compositional variation of m in the major families of inorganic network GFLs semi-quantitatively by relating the corresponding structural evolution and its temperature dependence with S_{conf} .

1. Introduction


The processing of glass products is critically dependent on the viscosity of the parent liquid and its variation with temperature.^[1] Typically, upon supercooling, the viscosity η of a glass-forming liquid (GFL), and hence its shear relaxation timescale τ_{shear} , increases by many orders of magnitude, and the activation energy of viscous flow increases in a non-Arrhenius manner.^[2] The degree of departure of the temperature dependence of η of a supercooled GFL from an Arrhenius behavior is often parameterized by the fragility index m , which is defined as $m = \left. \frac{d \log_{10} \eta}{d(T_g/T)} \right|_{T=T_g}$, where T_g represents the glass transition temperature.^[3] The quantity m has been shown to be a useful parameter for the classification of GFLs into “strong” and

2. Models, Results and Discussion

2.1. Chalcogenides—Disjointed Chains to Networks

Several studies in the literature have reported a sharp change in m as a function of the average network connectivity $\langle r \rangle$ across $\langle r \rangle \approx 2.3$ – 2.4 in a wide variety of chalcogenide GFLs.^[9,10] For example, the structure of liquid elemental Se consists of $-\text{Se}-\text{Se}-\text{Se}-$ chains with $\langle r \rangle = 2$ and is characterized by a rather high fragility index of $m \approx 80$. The addition of Ge and/or As to Se leads to a progressive increase in $\langle r \rangle$ as the Se chain segments get cross-linked via $\text{GeSe}_{4/2}$ tetrahedra or $\text{AsSe}_{3/2}$ pyramids. As $\langle r \rangle$ increases from 2 and approaches 2.4, m rapidly decreases to ≈ 30 , beyond which further increase in $\langle r \rangle$ up to the point of the stoichiometric composition GeSe_2 ($\langle r \rangle = 2.67$) results in negligible change in m (Figure 1) Sidebottom^[8] has shown that this variation in m versus $\langle r \rangle$ in these GFLs can be explained elegantly using a combination of the Adam–Gibbs configurational entropy model of relaxation and the self-avoiding walk (SAW) model of the conformational entropy of polymeric chains. As noted earlier, according to the Adam–Gibbs model, τ and hence η of a GFL increase exponentially with $1/(TS_{\text{conf}})$. Hence, by definition, m of a GFL is proportional to $\left. \frac{dS_{\text{conf}}}{dT} \right|_{T \rightarrow T_g} = \left(\frac{dS_{\text{conf}}}{d\langle r \rangle} \right) \cdot \left(\frac{d\langle r \rangle}{dT} \right) \Big|_{T \rightarrow T_g}$. The term $\left(\frac{d\langle r \rangle}{dT} \right)$ corresponds

S. Sen, H. Chen
Department of Materials Science & Engineering
University of California at Davis
Davis, CA 95616, USA
E-mail: sbsen@ucdavis.edu

 The ORCID identification number(s) for the author(s) of this article can be found under <https://doi.org/10.1002/pssb.202200002>.

DOI: 10.1002/pssb.202200002

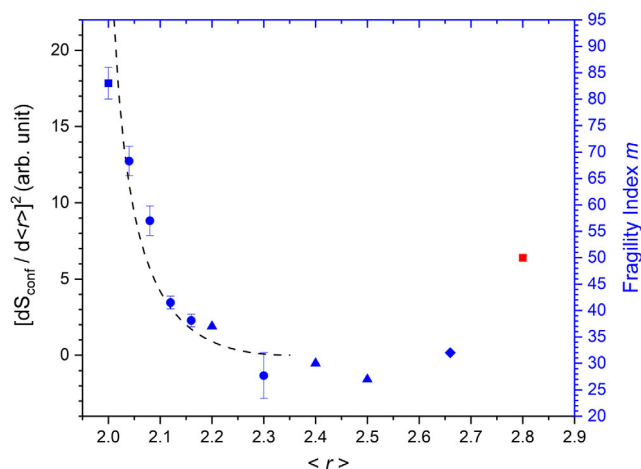


Figure 1. Comparison between the trend in the variation of $(\frac{dS_{\text{conf}}}{d(r)})^2$ calculated using the disjointed chain SAW model (dashed line) and experimentally determined fragility index m in Ge–Se system (filled symbols: blue circles,^[45] blue triangles,^[46] blue square,^[47] blue diamond,^[48] red square^[49]) as a function of $\langle r \rangle$.

to the temperature dependence of the average connectivity of the network, which is expected to be driven by configurational entropy and using the thermodynamics of a two-level system of broken versus intact bonds it can be shown that $(\frac{d(r)}{dT}) \propto (\frac{dS_{\text{conf}}}{d(r)})$ and hence $m \propto (\frac{dS_{\text{conf}}}{d(r)})^2$.^[8] The term $(\frac{dS_{\text{conf}}}{d(r)})$ represents the dependence of configurational entropy of a network on its connectivity, which, for chains with various degrees of cross-linking, has been investigated in detail in the polymer literature using the SAW model. Sidebottom^[8] used this model to estimate $\Delta S_{\text{SAW}} = (\frac{dS_{\text{conf}}}{d(r)})$, i.e., the change in the conformational entropy of a disjointed chain of monomers, upon progressive addition of cross-links, as a function of the length of the chain segments in between consecutive cross-links. The conformational entropy of a chain of 2-coordinated Se atoms can be approximated as a disjointed chain performing SAW,^[8] for which the number of possible conformations W of a chain of N monomers scales as $W \sim Z^N N^{-\delta}$, where $Z = 4.7$ and $\delta = 1.76$ in 3D. Consequently, it can be shown that the change in the conformational entropy of a disjointed chain of N Se atom monomers, upon progressive addition of $j-1$ cross-links, as a function of the length $L = N/j$ of the chain segments in between consecutive cross-links is given by^[8]

$$\Delta S_{\text{SAW}} = \left(\frac{dS_{\text{conf}}}{d(r)} \right) \approx -j\delta \ln\left(\frac{j}{j+1}\right) - \delta \ln\left(\frac{N}{j+1}\right) \quad (1)$$

This cross-linking scheme mimics the addition of Ge and/or As to Se in the structure of a chalcogenide GFL. We have used this model with $N \approx 200$ for pure Se to calculate the variation in $(\frac{dS_{\text{conf}}}{d(r)})^2$ along the Se–Ge join and a comparison between this quantity and the experimentally determined m values as a function of $\langle r \rangle$ for Se–Ge liquids is shown in Figure 1. Here, we ignore the possibility that the validity of the SAW expression

for W likely becomes questionable for L smaller than the persistence length of the chains, corresponding to a high degree of cross-linking. It must also be noted that the expression for the conformational entropy used here only accounts for that of isolated chains and does not include the collective effect of inter-chain interactions on the entropy, although the latter effect is expected to be significantly smaller than the former.^[11] However, despite these approximations, it is intriguing to note in Figure 1 the good qualitative agreement between the calculated and experimental m values as a function of $\langle r \rangle$ for liquids on the Se–Ge join in the range $2.0 \leq \langle r \rangle \leq 2.4$, lending support to Sidebottom's model.^[8]

Beyond this point, with further shortening of Se chain segments, their contribution to S_{conf} from the conformational entropy likely becomes insignificant compared to the temperature-dependent network reconfiguration “reactions.” Two such temperature-dependent “reactions” that have been studied in the literature in detail in the $\text{Ge}_x\text{Se}_{1-x}$ system using Raman spectroscopy are 1) the conversion of GeSe_4 tetrahedra between edge-shared and corner-shared geometry and 2) the conversion between homopolar and heteropolar bonds, e.g., $\text{Ge–Ge} + \text{Se–Se} \leftrightarrow 2(\text{Ge–Se})$.^[12,13] The latter reaction may, in fact, become a dominant source of temperature-dependent configurational entropy in chalcogen-deficient GFLs with an excess of Ge or As, which is consistent with the experimental observation that the m of Ge/As–Se networks increases with increasing connectivity in Se-deficient compositions (Figure 1).^[14] In fact, the m of $\text{As}_x\text{Se}_{100-x}$ GFLs starts to increase even for compositions with $x \geq 35$ as As–As homopolar bonds begin to appear in slightly Se-excess compositions.^[10] We emphasize the key role of such structural reactions in explaining the compositional variation of m in over-constrained oxide networks (vide infra). Moreover, local non-monotonic compositional variation of m in As and P chalcogenide GFLs has been related to the appearance of molecular units (e.g., As_4Se_3 , P_4Se_3 , and As_4S_3 units) over certain composition ranges, as such units can drastically lower the connectivity of a network as well as induce strong non-monotonic variation in various other physical properties.^[15]

2.2. Phosphates—the Inorganic Polymers

The structure of phosphate glasses is dominated by chains of corner-shared PO_4 tetrahedra over wide composition ranges and share a strong similarity in their rheological behavior with organic chain polymers.^[16] These similarities include experimental observations such as shear-induced crystallization and entropic shrinkage of phosphate chains that have been observed in phosphate liquids.^[17] Moreover, a recent study based on high-temperature ^{31}P NMR spectroscopy and rheometry has shown that phosphate chains do indeed behave like polymer chains in the sense that the reptation motion of these chains controls shear relaxation and viscous flow in metaphosphate liquids.^[18] Therefore, it may be argued that the SAW model of conformational entropy of disjointed chains could also be extended to model the fragility of phosphate GFLs along the metaphosphate– P_2O_5 join where the structural connectivity $\langle r \rangle$ now represents the connectivity of the phosphate network in terms of the number of bridging oxygen (BO) atoms per PO_4

tetrahedron in the structure.^[19] Here, the PO₄ tetrahedra are “coarse-grained” and treated as rigid super-structural units, which then do not contribute individually to the chain conformational entropy and only inter-tetrahedral conformational changes need to be considered for the estimation of entropy. Moreover, these rigid tetrahedral units do not undergo significant deformation in response to an applied shear; instead, the majority of the deformation is taken up by the linkages between these units.

However, such a model ignores the fact that while the conformational entropy of a chain of 2-coordinated Se atoms may be approximated as that of a disjointed chain performing SAW, the conformational entropy of a chain of tetrahedral units must be lower due to the excluded volume effect in addition to the steric constraints associated with tetrahedral rotation, and thus needs to be treated as a semiflexible chain performing a constrained SAW. Here, we adopt the definition for the term “semiflexible chain” from the polymer literature, where it denotes chains with bending stiffness that is large enough to successfully compete with their tendency for entropic coiling/folding. Further constraints for tetrahedral chain conformations in phosphate networks are introduced by the network-modifier cations, as high field strength modifiers such as Mg and Zn are known to provide stronger inter-chain coupling in metaphosphate GFLs, compared to their low field strength counterparts.^[20] Indeed, such constraints are manifested in the large variation in m shown by metaphosphate liquids, where it monotonically decreases with increasing field strength of the modifier cation (Figure 2).

Previous Monte Carlo simulation studies have shown that conformations of constrained chains follow the same scaling relation as that of a SAW, i.e., $W \sim Z^N N^{-\delta}$, except the parameter δ for the former becomes progressively lower as the chain motion becomes increasingly restricted.^[21,22] The corresponding variation in $\left(\frac{dS_{\text{conf}}}{d(r)}\right)^2$ versus $\langle r \rangle$ for a series of δ values ranging between 1.0 and 1.5, calculated using Equation (1), is shown in Figure 3

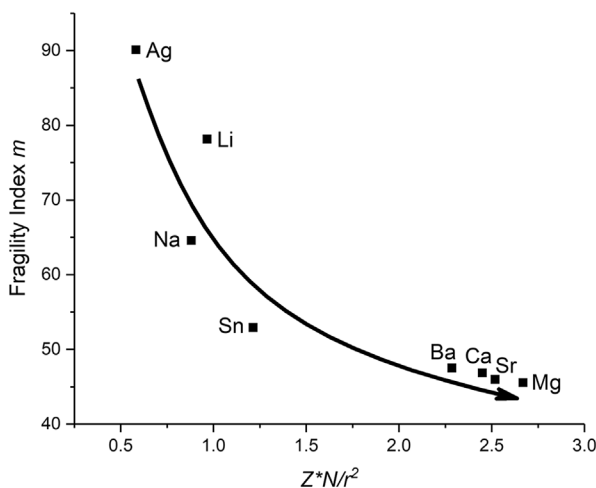


Figure 2. Fragility index m of various metaphosphate liquids as a function of modifier connectivity strength expressed as a product of field strength (Z/r^2) and coordination number N of the modifier cation. Z and r represent charge and average modifier-oxygen nearest-neighbor distance. Arrow showing trend is a guide to the eye. See a previous study^[20] for details and sources of data.

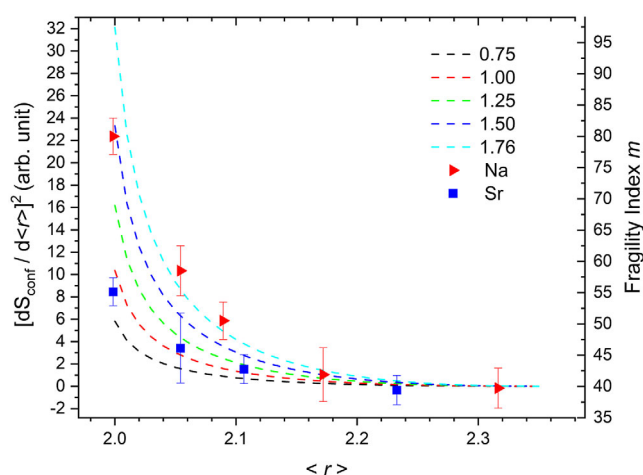


Figure 3. Fragility index m of SrO-P₂O₅ (blue squares) and Na₂O-P₂O₅ (red triangles) liquids determined in this study, as a function of tetrahedral connectivity $\langle r \rangle$. Dashed lines correspond to the variation in $\left(\frac{dS_{\text{conf}}}{d(r)}\right)^2$ with $\langle r \rangle$ in the SAW model for chains (dashed lines from bottom to top: $\delta = 0.75, 1.00, 1.25$, and 1.50 , respectively) and for disjointed chain (top-most dashed line: $\delta = 1.76$).

and compared with that for the SAW of a disjointed chain with $\delta = 1.76$. The results suggest that considering the proportionality between m and $\left(\frac{dS_{\text{conf}}}{d(r)}\right)^2$, as a network evolves from a 3D connected structure to a chain-like 2D structure, m would be expected to rise less rapidly for a network that is more constrained and vice versa. A comparison between these calculations and the m values of Na-phosphate and Sr-phosphate GFLs experimentally determined in this study indicates that while the behavior of the former GFLs corresponds to δ ranging between 1.76 and 1.5, that of the latter is best described by $\delta \approx 1.0$ (Figure 3). These results suggest that the constrained SAW model can explain the compositional variation in m for phosphate GFLs containing modifier cations with large differences in field strength. The high field strength Sr cations provide stronger constraints compared to the low field strength Na cations for phosphate networks with identical connectivity in the region with $2.0 \leq \langle r \rangle \leq 2.4$ (Figure 3). Further increase in $\langle r \rangle$ up to 3 for pure P₂O₅ results only in a small decrease in m .^[23]

2.3. Silicate and Aluminosilicate Networks—a Case for Percolation?

Silicate and aluminosilicate GFLs are archetypal examples of tetrahedral network liquids with corner-shared SiO₄ and AlO₄ tetrahedra. Unlike metaphosphate liquids, no coupling between chain reptation and viscous flow was observed in a high-temperature ²⁹Si NMR spectroscopic study of a silicate liquid close to the metasilicate composition (Na₄Si₃O₈).^[24] Rather, previous ²⁹Si and ¹⁷O dynamical NMR studies indicated that viscous flow and shear relaxation in silicate liquids are controlled by the Si–O bond scission-renewal process, which involves an exchange between the BO and non-bridging oxygen (NBO) environments.^[24,25] Therefore, it is not surprising that the

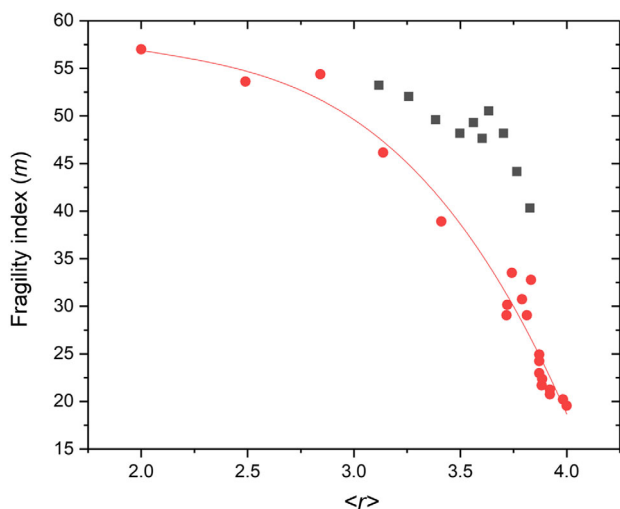


Figure 4. Fragility index m of compositions of multicomponent natural and synthetic silicate liquids (red circles), and Ca–Al–silicate liquids (black squares) as a function of tetrahedral connectivity $\langle r \rangle$.^[26,27] Solid red line through circles is a guide to the eye.

compositional variation of m versus $\langle r \rangle$ in these liquids follows a different pattern than that observed for chalcogenides and phosphates (Figures 1, 3, and 4). The m of silicate and aluminosilicate GFLs increases relatively rapidly as the NBO content increases and the inter-tetrahedral connectivity $\langle r \rangle$ decreases from 4 in SiO_2 to ≈ 3 –3.5 at the disilicate or tetrasilicate composition (Figure 4).^[26,27] Further increase in modifier content and consequent decrease in $\langle r \rangle$ result in little change in m down to the metasilicate composition with $\langle r \rangle = 2$ (Figure 4). This variation of m versus $\langle r \rangle$ is reminiscent of a percolative transition where the NBO content in the structure is sufficient for the dynamical percolation of mobile pathways for BO–NBO exchange that enables structural reconfiguration. Indeed, a number of previous studies have indicated that the temperature dependence of S_{conf} , and hence m in silicate liquids is likely dominated by the ability of oxygen atoms to explore new configurations and topological arrangements as volumetrically the oxygen sublattice dominates the structure of these liquids.^[28,29] The sharpness of this percolative transition, however, appears to be strongly system dependent as the Ca–Al–silicate liquids show a steeper rise in m with lowering of $\langle r \rangle$, while the natural alkali–alkaline-earth–Fe–Al silicate liquids display a more gradual transition (Figure 4). This attribute of the transition is likely controlled by the chemical interactions between the cations and the oxygen atoms that control the spatial distribution of the NBO atoms in the structure. Further systematic studies are needed in the future to address this issue from an atomistic standpoint.

2.4. Borate and Germanate Networks—a Resolution of the Apparent Anomaly

While for silicates and phosphates, the addition of a modifier oxide results in the formation of NBO atoms that lower the connectivity of the network, the borate and germanate networks respond quite differently, as unlike Si and P, the constituent

network-forming B and Ge cations can adopt multiple nearest-neighbor coordination states.^[30] Specifically, with the initial addition of network modifiers, the B–O coordination in borates increases from 3 to 4 and the Ge–O coordination in germanates increases from 4 to 5 and 6.^[30] Such an increase in the average coordination number increases the average connectivity of the network. Therefore, based on our experimental observation on silicates, phosphates, or chalcogenides as discussed earlier, one would expect that the initial addition of modifiers would result in a lowering of m in borate and germanate GFLs. However, experimentally m is observed to “anomalously” increase in alkali borates with up to 40 mol% alkali oxide and in alkali germanates with up to 20 mol% alkali oxide.^[31] It is important to note here that Vilgis proposed a model for the fragility of network liquids, where it was hypothesized that the compositional variation in m can be mapped onto the fluctuation of the coordination number of the network.^[32] In a recent study, Matsuda et al.^[33] tested this hypothesis by estimating the quenched fluctuation F in the boron coordination number Z in Li-borate glasses in terms of the weighted variance of the coordination number from the mean value \bar{Z} , which was expressed as $F = (3 - \bar{Z})^2 \cdot N_3 + (4 - \bar{Z})^2 \cdot N_4$, where $\bar{Z} = 3 \cdot N_3 + 4 \cdot N_4$ and N_3 and N_4 are the relative fractions of the 3- and 4-coordinated B atoms, respectively. These authors showed a remarkable one-to-one correlation between F and m in these networks.^[33] As the differential entropy of a structural variable is related to the variance of its probability distribution function, it is obvious that F can be related to S_{conf} . However, such a treatment does not explicitly include any temperature dependence of F , and thus considering $m \propto \frac{dS_{\text{conf}}}{dT} \big|_{T \rightarrow T_g}$, the origin of the observed correlation between m and F remains unclear. In contrast, previous studies over the last several decades have extensively investigated the effect of temperature on the coordination of B atoms in oxide glasses/liquids, where it has been demonstrated that increasing temperature shifts the equilibrium reaction $N_4 = N_3 + \text{NBO}$ to the right.^[34–38] Therefore, the temperature dependence of S_{conf} , and hence m must be closely related to this equilibrium fluctuation in the B coordination environment in borate liquids.^[34–38] It was shown that the approximate contribution of this boron speciation reaction to the change in the configurational heat capacity could be estimated by using the temperature dependence of the equilibrium constant K for the homogeneous reaction:^[35]

$$K = \frac{X[N_3][\text{NBO}]}{[N_4]} \quad (2)$$

where the terms in square brackets denote the concentrations of the different species involved in the speciation reaction and X is the ratio of the corresponding activity coefficients. The temperature dependence of K is given by the van’t Hoff relation:^[34]

$$\Delta H = -R \left[\frac{\ln K_1 - \ln K_2}{\frac{1}{T_1} - \frac{1}{T_2}} \right] \quad (3)$$

In this expression, ΔH is the enthalpy change associated with the speciation reaction, R is the gas constant, and K_1 and K_2 are the equilibrium constants for the reaction at two different

temperatures T_1 and T_2 . Therefore, ΔH for the speciation reaction can be calculated by approximating X to be temperature independent and by using the experimentally determined equilibrium concentrations of the N_3 , N_4 , and NBO species at two different temperatures T_1 and T_2 . Estimations of the corresponding contribution of this speciation reaction to the configurational heat capacity C_p^{conf} of alkali borate liquids were shown to be large enough to account for nearly the entire jump in C_p across glass transition.^[35–38]

Here, we have used Equation (2) and (3) to estimate the percentage N_f of B atoms that would undergo a change in their coordination number near T_g upon increasing the temperature from $T_g/T = 1$ to $T_g/T = 0.85$ in $(\text{Na}_2\text{O})_x(\text{B}_2\text{O}_3)_{1-x}$ glasses with alkali oxide contents of up to 30 mol%. The compositional variation in the $N_4:N_3$ ratio in these glasses was taken to be equal to^[39] $x/(1-x)$ and the NBO concentrations were taken from the thermodynamic speciation model of Ota et al.,^[40] which yields the percentage of BO_3 units with 1 NBO in this composition range whose composition dependence can be approximated by the expression $7.92x - 35.17x^2 + 271.88x^3$. The T_g of $(\text{Na}_2\text{O})_x(\text{B}_2\text{O}_3)_{1-x}$ glasses were taken from a previous report by Chrysikos et al.^[41] Finally, we have used a composition-independent value of $\Delta H = 45 \text{ kJ mol}^{-1}$ of B for the boron speciation reaction (see Equation (3)).^[34] The calculated compositional dependence of N_f is shown in **Figure 5** to be in good agreement with that of m in alkali borates, as reported by Chrysikos et al.^[42] Therefore, when taken together, these results clearly indicate an inextricable mechanistic connection between the $\frac{dS_{\text{conf}}}{dT}$ associated with the temperature dependence of the boron coordination environment and m in borate GFLs.

Although detailed data on the temperature dependence of structural speciation are not available, a similar argument can also be made for the germanate GFLs, where, similar to borates, m increases with the initial addition of alkali oxide network

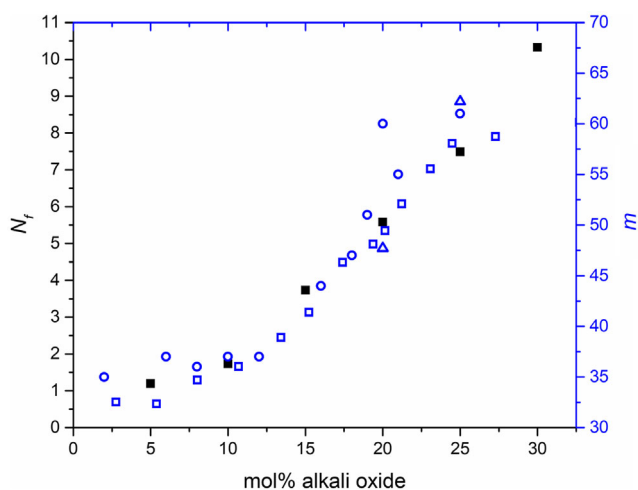


Figure 5. Comparison between the trends in the compositional variation of calculated values of N_f (solid squares, see text for details) and experimentally determined fragility index m (open symbols) in alkali borate systems. Open squares, circles, and triangles correspond to m of sodium borate, lithium borate, and potassium borate liquids, respectively, determined in previous studies.^[40,42,50]

modifiers despite increased connectivity of the network via an increase in the Ge–O coordination number. In fact, recent Raman spectroscopic studies have indicated a temperature-dependent Ge speciation in $\text{K}_2\text{O–GeO}_2$ GFLs that can be expressed as $\text{GeO}_6^{2-} \cdot 2\text{M}^+ + \text{GeO}_4 \leftrightarrow 2(\text{GeO}_3\text{O}^- \cdot \text{M}^+)$, where O and O represent bridging and NBO atoms, respectively.^[43] We argue that, similar to borates, such structural speciation reactions can act as an important source of $\frac{dS_{\text{conf}}}{dT}$ in germanates, which can explain the apparently anomalous compositional trends of m in networks where the constituent network-forming cations can assume multiple coordination environments with relative ease.

3. Conclusions

The chalcogenide and phosphate GFLs display a relatively rapid drop in the fragility index m with increasing connectivity $\langle r \rangle$ in the region $2.0 \leq \langle r \rangle \leq 2.4$, beyond which m does not show any significant variation with composition. The decreasing trend in m in the region $2.0 \leq \langle r \rangle \leq 2.4$ can be related to the lowering in $\left(\frac{dS_{\text{conf}}}{dT}\right)^2$ with progressive cross-linking of the constituent chain-like elements in these liquids as $\langle r \rangle$ increases beyond 2.0. The differences in the rate of change of m with $\langle r \rangle$ in phosphate versus chalcogenide liquids can be ascribed to the corresponding dissimilarities in the relative bending stiffness of the constituent chain-like elements. The bending stiffness appears to be the lowest for chains of 2-coordinated chalcogen atoms, which behave as disjointed chains performing SAW resulting in a sharp rise in m as $\langle r \rangle$ approaches 2.0 in chalcogenides. In comparison, m rises less rapidly with decreasing $\langle r \rangle$ in phosphate liquids, indicating that a chain of tetrahedral PO_4 units needs to be treated as semiflexible with a higher bending stiffness, performing constrained SAW. The field strength of the modifier cation is shown to have a similar effect on the effective bending stiffness of the constituent phosphate chain elements as cations with higher field strength provide stronger inter-chain coupling, thus increasing the effective stiffness of these chains and lowering their conformational entropy. Although m increases with decreasing $\langle r \rangle$ in silicate and aluminosilicate GFLs, the variation displays a pattern that is fundamentally different compared to that in chalcogenide and phosphate GFLs and is suggestive of S_{conf} being controlled by structural rearrangements in a dynamically percolative oxide network via NBO–BO chemical exchange. In contrast to chalcogenide, silicate, and phosphate liquids, m increases with increasing $\langle r \rangle$ in borate and germanate liquids. This apparently anomalous trend in m versus $\langle r \rangle$ in borate liquids is shown to be related to the fact that upon addition of modifier cations to B_2O_3 , the network-forming B atoms adopt multiple coordination states and their relative fractions become dependent on temperature. Consequently, temperature-dependent speciation reactions such as $\text{BO}_4 \leftrightarrow \text{BO}_3 + \text{NBO}$ act as the dominant source of $\frac{dS_{\text{conf}}}{dT}$ and control the composition dependence of m in these liquids. A similar scenario is suggested for germanate liquids via the recently observed temperature-dependent speciation reaction: $\text{GeO}_6^{2-} \cdot 2\text{M}^+ + \text{GeO}_4 \leftrightarrow 2(\text{GeO}_3\text{O}^- \cdot \text{M}^+)$.

4. Experimental Section

The calorimetric fragility index m of $(\text{Na}_2\text{O})_x(\text{P}_2\text{O}_5)_{100-x}$ and $(\text{SrO})_x(\text{P}_2\text{O}_5)_{100-x}$ glasses were determined in this study. These glasses were prepared by the conventional melt-quenching method. The fragility index m of these phosphate glasses was determined using differential scanning calorimetry (Mettler Toledo DSC1). Samples of mass $\approx 15\text{--}20$ mg were taken in hermetically sealed Al pans and were heated to 50°C above T_g to erase any thermal history. The samples were then cooled in the calorimeter at a rate of 10 K min^{-1} and subsequently reheated at the same rate. The fictive temperature T_f was taken as the peak of the endothermic glass transition signal while heating the sample at a specific rate q ranging from 0.5 to 30 K min^{-1} , subsequent to cooling at the same rate from $T_g + 30\text{ K}$ to $T_g - 50\text{ K}$. The T_g was determined to within $\pm 2^\circ\text{C}$ as the onset of the glass transition endotherm at a heating rate of 10 K min^{-1} . On the other hand, the dependence of T_f on q yields the activation energy E for enthalpy relaxation according to the relation:

$$\frac{d \ln q}{d \left(\frac{1}{T_g} \right)} = - \frac{E}{R} \quad \text{The fragility index } m \text{ was determined from } E \text{ using the relation}$$

$$m = \frac{E}{RT_g \ln 10} \quad [44]$$

Acknowledgements

This work was supported by the National Science Foundation Grant NSF-DMR 1855176. S.S. acknowledges the support from the Blacutt-Underwood Professorship grant at UC Davis.

Conflict of Interest

The authors declare no conflict of interest.

Data Availability Statement

The data that support the findings of this study are available from the corresponding author upon reasonable request.

Keywords

configurational entropy, fragility, inorganic glass-forming liquids, network connectivity

Received: January 3, 2022
Revised: February 2, 2022
Published online:

- [1] Q. Zheng, J. C. Mauro, A. J. Ellison, M. Potuzak, Y. Yue, *Phys. Rev. B* **2011**, *83*, 212202.
- [2] A. Cavagna, *Phys. Rep.* **2009**, *476*, 51.
- [3] C. A. Angell, *J. Non-Cryst. Solids* **1991**, *131*, 13.
- [4] G. Adam, J. H. Gibbs, *J. Chem. Phys.* **1965**, *43*, 139.
- [5] J. Dudowicz, J. F. Douglas, K. F. Freed, *J. Chem. Phys.* **2014**, *141*, 234903.
- [6] V. Lubchenko, P. G. Wolynes, *Annu. Rev. Phys. Chem.* **2007**, *58*, 235.
- [7] E. A. Di Marzio, A. J. M. Yang, *J. Res. Natl. Inst. Stand. Technol.* **1997**, *102*, 135.
- [8] D. L. Sidebottom, *Phys. Rev. E: Stat. Nonlin. Soft Matter Phys.* **2015**, *92*, 1.
- [9] S. Sen, Y. Xia, W. Zhu, M. Lockhart, B. Aitken, *J. Chem. Phys.* **2019**, *150*, 144509.
- [10] Y. Xia, B. Yuan, O. Gulbitten, B. Aitken, S. Sen, *J. Phys. Chem. B* **2021**, *125*, 2754.
- [11] C. P. Broedersz, F. C. Mackintosh, *Rev. Mod. Phys.* **2014**, *86*, 995.
- [12] B. Yuan, H. Chen, S. Sen, *J. Phys. Chem. B* **2022**, *126*, 946.
- [13] T. G. Edwards, S. Sen, *J. Phys. Chem. B* **2011**, *115*, 4307.
- [14] A. Zeidler, P. S. Salmon, D. A. J. Whittaker, K. J. Pizzey, A. C. Hannon, *Front. Mater.* **2017**, *4*, 32.
- [15] D. C. Kaseman, I. Hung, Z. Gan, B. Aitken, S. Currie, S. Sen, *J. Phys. Chem. B* **2014**, *118*, 2284.
- [16] J. U. Otaigbe, G. H. Beall, *Trends Polym. Sci.* **1997**, *11*, 369.
- [17] S. Inaba, H. Hosono, S. Ito, *Nat. Mater.* **2015**, *14*, 312.
- [18] Y. Xia, W. Zhu, J. Sen, S. Sen, *J. Chem. Phys.* **2020**, *152*, 044502.
- [19] D. L. Sidebottom, S. E. Schnell, *Phys. Rev. B* **2013**, *87*, 054202.
- [20] Y. Xia, W. Zhu, M. Lockhart, B. Aitken, S. Sen, *J. Non-Cryst. Solids* **2019**, *514*, 77.
- [21] J. Douglas, C. M. Guttman, A. Mah, T. Ishinabe, *Phys. Rev. E* **1997**, *55*, 738.
- [22] A. E. Van Giessen, I. Szleifer, *J. Chem. Phys.* **1995**, *102*, 9069.
- [23] D. L. Sidebottom, J. R. Changstrom, *Phys. Rev. B* **2008**, *77*, 020201(R).
- [24] J. F. Stebbins, S. Sen, I. Farnan, *Am. Miner.* **1995**, *80*, 861.
- [25] S. Sen, *Prog. Nucl. Magn. Reson. Spectrosc.* **2020**, *116*, 155.
- [26] D. Giordano, D. B. Dingwell, *J. Phys.: Condens. Matter* **2003**, *15*, S945.
- [27] M. Moesgaard, Y. Yue, *J. Non-Cryst. Solids* **2009**, *355*, 867.
- [28] P. Richet, D. R. Neuville, in *Thermodynamic Data: Systematics and Estimation*, Advances in Physical Geochemistry, Vol. 10 (Ed: S. Saxena), Springer-Verlag, Berlin **1992**, pp. 132–160.
- [29] M. J. Toplis, D. B. Dingwell, K. U. Hess, T. Lenci, *Am. Miner.* **1997**, *82*, 979.
- [30] J. F. Stebbins, J. Wu, L. M. Thompson, *Chem. Geol.* **2013**, *346*, 34.
- [31] D. L. Sidebottom, T. D. Tran, S. E. Schnell, *J. Non-Cryst. Solids* **2014**, *402*, 16.
- [32] T. A. Vilgis, *Phys. Rev. B* **1993**, *47*, 2882.
- [33] Y. Matsuda, Y. Fukawa, M. Kawashima, S. Mamiya, S. Kojima, *Solid State Ionics* **2008**, *179*, 2424.
- [34] J. F. Stebbins, S. E. Ellsworth, *J. Am. Ceram. Soc.* **1996**, *79*, 2247.
- [35] S. Sen, Z. Xu, J. F. Stebbins, *J. Non-Cryst. Solids* **1998**, *226*, 29.
- [36] S. Sen, *J. Non-Cryst. Solids* **1999**, *253*, 84.
- [37] L. Cormier, O. Majerus, D. R. Neuville, G. Calas, *J. Am. Ceram. Soc.* **2006**, *89*, 13.
- [38] O. Majerus, L. Cormier, G. Calas, B. Beuneu, *Phys. Rev. B* **2003**, *67*, 024210.
- [39] J. Zhong, P. J. Bray, *J. Non-Cryst. Solids* **1989**, *111*, 67.
- [40] R. Ota, T. Yasuda, J. Fukunaga, *J. Non-Cryst. Solids* **1990**, *116*, 46.
- [41] G. D. Chrysikos, J. A. Duffy, J. M. Hutchinson, M. D. Ingram, E. I. Kamitsos, A. J. Pappin, *J. Non-Cryst. Solids* **1994**, *172–174*, 378.
- [42] G. D. Chrysikos, E. I. Kamitsos, Y. D. Yiannopoulos, *J. Non-Cryst. Solids* **1996**, *196*, 244.
- [43] O. N. Koroleva, A. A. Osipov, *J. Non-Cryst. Solids* **2020**, *531*, 119850.
- [44] S. Wei, G. J. Coleman, P. Lucas, C. A. Angell, *Phys. Rev. Appl.* **2017**, *7*, 034035.
- [45] R. Svoboda, J. Málek, *J. Non-Cryst. Solids* **2015**, *419*, 39.
- [46] Y. Gueguen, T. Rouxel, P. Gadaud, C. Bernard, V. Keryvin, J. C. Sangleboeuf, *Phys. Rev. B* **2011**, *84*, 064201.
- [47] P. Košťál, J. Málek, *J. Non-Cryst. Solids* **2010**, *356*, 2803.
- [48] L. Orsingher, G. Baldi, A. Fontana, L. E. Bove, T. Unruh, A. Orecchini, C. Petrillo, N. Violini, F. Sacchetti, *Phys. Rev. B* **2010**, *82*, 115201.
- [49] U. Senapati, A. K. Varshneya, *J. Non-Cryst. Solids* **1996**, *197*, 210.
- [50] M. Luis Ferreira Nascimento, C. Aparicio, *J. Phys. Chem. Solids* **2007**, *68*, 104.